

Geology

Middle Miocene reorganization of deformation along the northeastern Tibetan Plateau

Richard O. Lease, Douglas W. Burbank, Marin K. Clark, Kenneth A. Farley, Dewen Zheng and Huiping Zhang

Geology 2011;39:359-362
doi: 10.1130/G31356.1

Email alerting services click www.gsapubs.org/cgi/alerts to receive free e-mail alerts when new articles cite this article

Subscribe click www.gsapubs.org/subscriptions/ to subscribe to *Geology*

Permission request click <http://www.geosociety.org/pubs/copyrt.htm#gsa> to contact GSA

Copyright not claimed on content prepared wholly by U.S. government employees within scope of their employment. Individual scientists are hereby granted permission, without fees or further requests to GSA, to use a single figure, a single table, and/or a brief paragraph of text in subsequent works and to make unlimited copies of items in GSA's journals for noncommercial use in classrooms to further education and science. This file may not be posted to any Web site, but authors may post the abstracts only of their articles on their own or their organization's Web site providing the posting includes a reference to the article's full citation. GSA provides this and other forums for the presentation of diverse opinions and positions by scientists worldwide, regardless of their race, citizenship, gender, religion, or political viewpoint. Opinions presented in this publication do not reflect official positions of the Society.

Notes

Middle Miocene reorganization of deformation along the northeastern Tibetan Plateau

Richard O. Lease^{1*}, Douglas W. Burbank¹, Marin K. Clark², Kenneth A. Farley³, Dwen Zheng⁴, and Huiping Zhang⁴

¹Department of Earth Science, University of California–Santa Barbara, Santa Barbara, California 93106, USA

²Department of Geological Sciences, University of Michigan, Ann Arbor, Michigan 48109, USA

³Division of Geological and Planetary Sciences, California Institute of Technology, Pasadena, California 91125, USA

⁴State Key Laboratory of Earthquake Dynamics, Institute of Geology, China Earthquake Administration, Beijing 100029, China

ABSTRACT

Temporal variations in the orientation of Cenozoic range growth in northeastern Tibet define two modes by which India-Asia convergence was accommodated. Thermochronological age-elevation transects from the hanging walls of two major thrust-fault systems reveal diachronous Miocene exhumation of the Laji-Jishi Shan in northeastern Tibet. Whereas accelerated growth of the WNW-trending eastern Laji Shan began ca. 22 Ma, rapid growth of the adjacent, north-trending Jishi Shan did not commence until ca. 13 Ma. This change in thrust-fault orientation reflects a Middle Miocene change in the kinematic style of plateau growth, from long-standing NNE-SSW contraction that mimicked the plate convergence direction to the inclusion of new structures accommodating east-west motion. This kinematic shift in northeastern Tibet coincides with expansion of the plateau margin in southeastern Tibet, the onset of normal faulting in central Tibet, and accelerated shortening in northern Tibet. Together these phenomena suggest a plateau-wide reorganization of deformation.

INTRODUCTION

The indentation of a weak continent by a strong one is accommodated in the upper crust by fault slip that thickens and translates the crust. During the early stages of orogenesis, collision is commonly manifest by the development of thrust faults oriented orthogonally to the convergence direction. With continued convergence over many millions of years, however, the geometry and kinematics of faulting become more complex (Dewey, 1988). Thrust faults in highly evolved collisional orogenic plateaus are oriented both parallel and perpendicular to the plate convergence direction and can be active concurrently with strike-slip and normal faults, as evinced by the modern Tibetan Plateau (Molnar and Lyon-Caen, 1989).

The emergence of new fault systems of variable orientation or type signifies a change in strain partitioning. In particular, lateral movement of crustal material orthogonal to plate convergence direction may be a natural evolutionary stage for collisional orogenic plateaus as an expression of (1) orogenic collapse and the outward transfer of gravitational potential energy (Dewey, 1988), and/or (2) heterogeneities in lithospheric strength whereby crustal material becomes pinned against a more rigid backstop and deformation migrates toward unconfined lateral margins (Tapponnier et al., 1982). Even when evidence exists for such an overall evolution, however, the timing of the change in deformation patterns and its position within the evolutionary succession are commonly unknown.

The Tibetan-Himalayan orogen provides a valuable natural laboratory for examining the kinematics of continental deformation driven by continent-continent collision. Here we present thermochronological data that reveal a diachronous onset of NNE-vergent versus east-vergent thrust faulting along the northeastern Tibetan Plateau. Paired apatite (U-Th)/He and fission-track ages from two nearby age-elevation transects in the Laji-Jishi Shan show that the range is a composite structure in which Early Miocene NNE-SSW shortening of the Laji Shan was followed by Middle to Late Miocene east-west shortening of the adjacent Jishi Shan.

GEOLOGICAL SETTING

The Tibetan-Himalayan orogen has accommodated >1400 km of north-south shortening since early Cenozoic time (Yin and Harrison, 2000) during a prolonged period of contraction parallel to the plate convergence direction. Contraction commenced on the northern plateau margin (Yin et al., 2002) within a few million years of initial India-Asia continental collision ca. 50 Ma (Rowley, 1996), and implies a rapid transfer of stress over the >3000 km distance separating northern Tibet from the plate boundary at that time (Molnar and Stock, 2009). On the northeastern margin of the plateau, early Cenozoic deformation was accommodated primarily by WNW-trending thrust faults such as the West Qinling fault, where the onset of rapid cooling ca. 45–50 Ma indicates initial thrusting (Fig. 1; Clark et al., 2010).

In contrast to early Cenozoic contraction that was primarily oriented parallel to the plate convergence direction, the present kinematic field

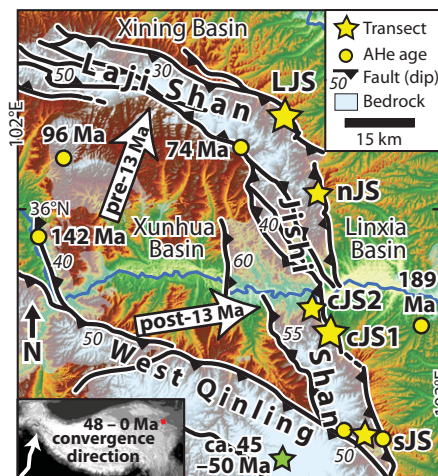


Figure 1. Laji Shan–Jishi Shan map with thermochronology transect and sample locations shown. Note change from WNW-trending thrust faults in Laji Shan and West Qinling to north-trending thrust faults in Jishi Shan. White arrows indicate primary contraction orientation (bidirectional) in this area before and after ca. 13 Ma, as suggested by our thermochronological data (see Figs. 2 and 3). Age-elevation transects: LJS—Laji Shan; cJS1, cJS2—Jishi Shan central; nJS—Jishi Shan north; sJS—Jishi Shan south. West Qinling vertical transect (green star) is from Clark et al. (2010). Areas not shaded as bedrock have Cenozoic basin fills that have been incised by Yellow River flowing from west to east. Arrow in inset location map points toward azimuth of northward motion of Indian plate with respect to Eurasian plate since 48 Ma (Molnar and Stock, 2009). Fault attitudes modified from Qinghai Bureau of Geology and Mineral Resources (1991).

in northeastern Tibet is more complex and characterized by both dextral and sinistral strike-slip faulting, as well as contraction along WNW-trending and north-trending thrust faults (Duvall and Clark, 2010, and references therein). North-trending thrust faults that accommodate lateral motion initiated by ca. 8 Ma in the Liupan Shan (Zheng et al., 2006). The nature and timing of this change in contraction direction, however, remain poorly understood: most ranges in northern and eastern Tibet typically record either NNE-SSW or east-west contraction, but seldom both. The 10–25-km-wide Laji-Jishi Shan rise to elevations >4000 m and tower above the

*E-mail: rlease@crustal.ucsb.edu.

adjacent Yellow River at ~2000 m elevation (Fig. 1). Both WNW-trending thrust faults of the Laji Shan and north-trending thrust faults of the Jishi Shan place early Paleozoic, Cretaceous, and Proterozoic basement rocks over Cenozoic fluvio-lacustrine sedimentary strata that are 1–3 km thick (Qinghai Bureau of Geology and Mineral Resources, 1991).

METHODS

Low-temperature thermochronology tracks the cooling history of the shallow crust at ~2–5 km depth and records thermal perturbations caused by fault-induced increases in erosion rate. We utilize the elevation dependency of apatite (U-Th)/He (AHe) and apatite fission-track (AFT) ages, with respective closure temperatures of ~60–70 °C (Flowers et al., 2009) and ~100–110 °C (Ketcham et al., 2007), to determine the onset and duration of accelerated thrust-related exhumation.

In order to delineate a cooling history related to thrust displacement, we collected samples from steep topographic transects within the hanging walls of two major thrust faults that are oriented nearly orthogonal to one another (Fig. 1). We collected 8 samples (8 AHe ages, 5 AFT ages) from a single transect on the hanging wall of the NNE-vergent Laji Shan thrust and 19 samples (16 AHe ages, 10 AFT ages) from the hanging wall of the east-vergent Jishi Shan thrust (Fig. 2). Although most of the Jishi Shan samples were collected from a single transect in the central portion of the range (Fig. 2B), three shorter transects along strike of the range front were also sampled (Fig. 1). In the absence of structural or geomorphic horizons in the vicinity of our samples, we interpret the steeply dipping faults (40°–60°; Fig. 1) and associated long (>10 km), gently dipping (<10°) backlimbs nearby to suggest that the hanging wall has moved vertically without internal deformation, and thus elevation is a proxy for depth. In addition, in order to examine larger patterns of exhumation, we collected footwall samples from outcrops in adjacent basins.

We used the forward-modeling function in HeFTy 1.6.7.43 (Ketcham, 2005) to predict cooling ages for various monotonic time-temperature histories that tested a range of onset times of rapid cooling, diverse cooling rates, and changes in rates through time. These models were then compared to our data to determine a preferred thermal history that was consistent with all of the ages from a particular mountain range. (See the GSA Data Repository¹ for

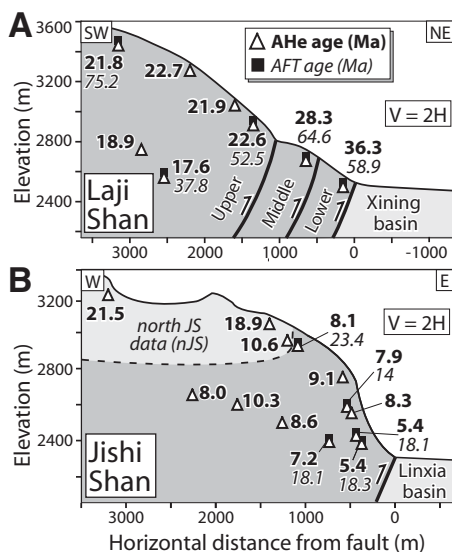


Figure 2. Apatite (U-Th)/He (AHe) and apatite fission-track (AFT) cooling ages on simplified geological cross sections. A: Laji Shan. B: Jishi Shan. Of 13 Jishi Shan samples, 10 are from central Jishi Shan with 3 high-elevation samples projected from 30 km to north (nJS). In upper thrust block in both Laji Shan and central Jishi Shan, narrow range of AHe ages indicates rapid cooling by time of AHe closure ca. 22 Ma and ca. 10 Ma, respectively. Upper, middle, and lower thrust faults interpreted from cooling ages and local geology; 2× vertical exaggeration. AHe and AFT analytical information is in Tables DR1–DR4 in the Data Repository (see footnote 1).

a more detailed description of analytical and modeling methods.)

RESULTS

Extensive Neogene exhumation in our study area was limited to localized erosion of the Laji Shan and Jishi Shan, where rocks with Miocene AHe cooling ages are exposed (Fig. 2). These Miocene ages contrast with those from bounding basins and nearby ranges adjacent to the Laji and Jishi Shan that contain basement samples with a wide range of Mesozoic ages (189 Ma to 96 Ma; Fig. 1) consistent with slow regional pre-Cenozoic cooling.

In geological cross section, cooling ages are interpreted to reveal the Laji Shan range-bounding thrust system as comprising multiple faults (Fig. 2A). Spanning a distance of ~1–3 km from the range-bounding thrust and 900 m of relief, the 6 samples from the Laji Shan interior (e.g., upper thrust block, Fig. 2A) have internally consistent ca. 18–23 Ma AHe ages. This coherent pattern of ages suggests a shared cooling history as a single hanging-wall block. Our 2 samples within 1 km distance of the range front and at low elevations, however, have older ca. 28–36 Ma AHe ages over <200 m of relief (Fig. 2A). Collectively, Laji Shan samples on a

3-km-long horizontal transect perpendicular to the range front at ~2600 m elevation display an 18 m.y. dichotomy in AHe ages. In the context of the consistent Early Miocene cooling trend in the range interior, this incongruity suggests that imbricate faults cut the flank of the range in a hindward-breaking thrust sequence (Fig. 2A). Alternative structural interpretations for the Laji Shan, such as a fold forelimb, are inconsistent with the geometry of AHe and AFT ages and still require an Early Miocene transition to accelerated cooling. When interpreting the Cenozoic cooling history of the Laji Shan, we therefore focus on the consistent thermochronometer ages from the upper thrust block in the range interior. Whereas thermochronometer ages from the upper thrust block vary linearly with elevation, ages do not scale with relative height above the fault plane (Fig. 2A). This geometry suggests a hanging-wall ramp on footwall ramp structural geometry with <5° of back tilting.

AHe/AFT age-elevation relationships from the Laji Shan interior reveal the onset of accelerated exhumation ca. 22 Ma (Fig. 3A) which we infer to be a response to NNE-SSW contraction on the range-bounding thrust. Spanning 900 m of relief, AFT ages from the hanging wall of the Laji Shan upper thrust fault systematically decrease from 75.2 to 37.8 Ma with decreasing elevation. These AFT age-elevation data suggest very slow cooling within an early Cenozoic partial annealing zone. AHe samples from the same transect, however, have more restricted ages that range from 22.7 to 17.6 Ma (Fig. 3A). When compared to the 37 m.y. range of AFT ages for minerals from the same samples and vertical transect, this 5 m.y. span of AHe ages indicates a transition to relatively rapid cooling by the time of AHe closure. In particular, the upper 600 m of the AHe vertical transect comprises 4 samples that differ in age by <1 m.y., ranging from 22.7 to 21.8 Ma. This consistency is interpreted to signal the onset of rapid cooling by ca. 22 Ma (Fig. 3A). The 37 m.y. range of AFT ages on the upper thrust block together with the large 20–53 m.y. difference between all paired AFT and AHe ages from individual samples suggest relatively slow rates of cooling (<1 °C/m.y.) during the early Cenozoic throughout the Laji Shan sampled domain.

Our forward models predict thermal histories that can be assessed against our entire suite of age-elevation data (Fig. 3). Because the close spatial proximity of our samples requires a thermal history that is consistent with all of our data, we prefer the more holistic forward-model approach to the more commonly used inverse models of individual samples (Ketcham, 2005). The model results (Fig. 3A) suggest that the Laji Shan underwent ~60 °C of rapid cooling starting ca. 22 Ma after a prolonged period of isothermal holding since the

¹GSA Data Repository item 2011119, thermochronological methods and data, is available online at www.geosociety.org/pubs/ft2011.htm, or on request from editing@geosociety.org or Documents Secretary, GSA, P.O. Box 9140, Boulder, CO 80301, USA.

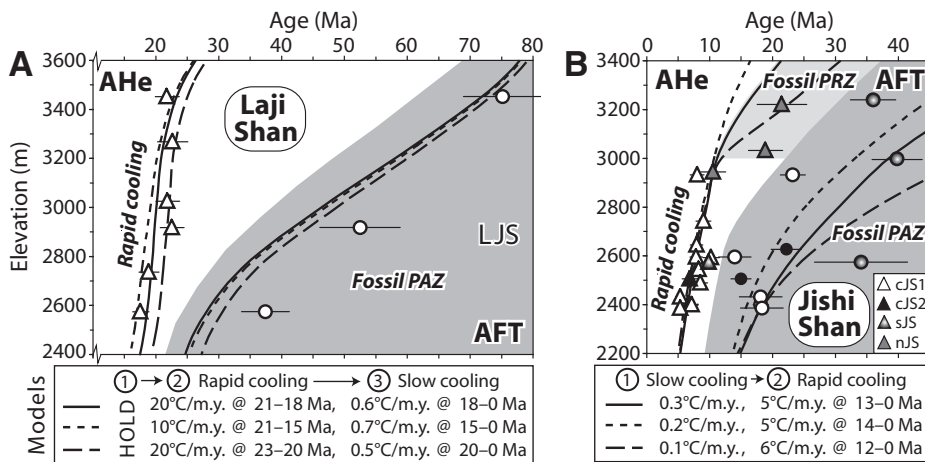


Figure 3. Age-elevation relationships and cooling model results for apatite (U-Th)/He (AHe; triangle) and apatite fission-track (AFT; circle) samples from hanging walls of thrust faults. A: Laji Shan. B: Jishi Shan. Samples from similar elevations in each respective range display wide range of AFT ages indicative of slow Paleogene cooling within fossil partial annealing zone (PAZ) and narrow range of AHe ages suggestive of rapid cooling starting in Miocene time, except AHe samples from northern Jishi Shan (>3000 m), which may capture base of fossil partial retention zone (PRZ). Gray shading highlights samples within interpreted PAZ and PRZ. Note pulses of rapid cooling ca. 22 Ma in WNW-trending Laji Shan and ca. 13 Ma in north-trending Jishi Shan. Of 25 Jishi Shan ages, 17 are from single transect (cJS1) with 8 ages projected along strike of range front (see Fig. 1 for locations and abbreviations). Laji Shan ages were forward modeled (Ketchum, 2005) with three successively younger cooling segments, (1) pre-Miocene isothermal holding, (2) rapid cooling over a defined interval, and (3) slower cooling, whereas Jishi Shan ages were modeled with two cooling segments, (1) slow initial cooling, and (2) rapid subsequent cooling. Geothermal gradients of 25 °C/km (Jishi Shan) and 20 °C/km (Laji Shan) allow thermal histories to be cast in age-elevation space and are in agreement with surface heat flow measurements (Hu et al., 2000). Our preferred model runs closely predicted AHe ages and are consistent with less precise AFT ages. We ignore advection of isotherms (for rationale, consult the Data Repository [see footnote 1]).

Early Cretaceous. Our preferred model suggests rapid cooling at a rate of 10–20 °C/m.y. from 23–21 Ma until 20–15 Ma, followed by slow cooling at a rate of ~0.6 °C/m.y. from 20–15 Ma until the present (Fig. 3A), representing peak erosion rates of 0.5–1 mm/yr followed by 0.03 mm/yr, respectively.

In contrast to accelerated exhumation starting ca. 22 Ma above the NNE-vergent Laji Shan thrust, accelerated exhumation of the Jishi Shan due to east-west contraction did not commence until Middle Miocene time (Fig. 3B). Samples from common elevations of <3000 m along the Jishi Shan range front have similar Late Miocene AHe ages and suggest that equivalent structural depths are exposed along the range front: these samples can therefore be projected onto a composite age-elevation section (Fig. 3B). The 13 AHe samples that span the lowest 550 m of relief on the hanging wall of the Jishi Shan thrust fault have a narrow range of ages limited to 10.6–5.4 Ma (most ages between 9 and 7 Ma), indicating that the Jishi Shan was cooling rapidly by the Late Miocene. The AHe samples from an overlying 300 m increment of relief, however, have a wider, 11 m.y., span of ages and decrease from 21.5 to 10.6 Ma with decreasing elevation, indicating an Early to Middle Miocene period of slower

cooling (Fig. 3B). Furthermore, AFT samples from the same 850 m span of relief on the Jishi Shan hanging wall have a broad 26 m.y. range in ages, from ca. 40 to 14 Ma, and suggest slow Eocene–Middle Miocene cooling (Fig. 3B). Collectively, the Jishi Shan AHe age-elevation relationship captures a Middle Miocene acceleration in cooling rate which is reinforced by AFT data that are scattered, but indicative of slow cooling until this time (Fig. 3B). Forward modeling of our entire Jishi Shan AFT and AHe age-elevation data set (26 ages) indicates that the range underwent ~70 °C of relatively rapid cooling from ca. 13 Ma until the present at a rate of 5–6 °C/m.y., with slow cooling before ca. 13 Ma at a rate of 0.1–0.3 °C/m.y. (Fig. 3B), representing erosion rates of ~0.2 mm/yr and ~0.01 mm/yr, respectively.

DISCUSSION

Our AFT data sets in both the Laji Shan and Jishi Shan display a wide, ~30 m.y. range of ages over limited relief (<1 km) that strongly suggests slow rock cooling in the Paleogene (Fig. 3). Many of these AFT samples, however, have measured mean track lengths that are long (>14 μm; see the Data Repository) and imply rapid cooling, a result that contradicts the age-elevation trends. We argue that a holistic view

of the entire suite of AFT, as well as of AHe ages and altitudes, yields the most appropriate interpretation of the cooling history for each range given: (1) the requirement for a coherent exhumation history that explains all of the cooling ages within the entire hanging wall block, (2) the close spatial proximity of most samples (<2 km apart in map view; Fig. 2), and (3) the consistent age-elevation trends (Fig. 3). Thus, we favor the age-elevation data, which summarize multiple thermochronometers from several different samples collected over ~1 km of relief, and we do not consider track lengths from individual samples in our analysis.

In our forward models, we search for preferred solutions to our entire age-elevation data sets with particular focus on the AHe data. Imperfect fits are expected with such forward models, especially when samples have different kinetic properties, e.g., effective uranium or etch figure diameter D_{par} , and thus slightly different closure temperatures, as well as when data are projected from >10 km away onto a single age-elevation array (as done for some Jishi Shan ages). Despite these caveats, our data are tightly clustered and yield readily defined intervals of accelerated cooling (Fig. 3).

Our data show a significant change in the orientation of thrust faulting in Miocene time despite limited exhumation and only incremental expansion of the plateau margin during that time (Clark et al., 2010). We identify three episodes in the Cenozoic contractional history of northeastern Tibet centered near 36°N, 102.5°E (Fig. 1). First, a protracted period of NNE-SSW contraction commenced ca. 45–50 Ma in the West Qinling (Clark et al., 2010). Second, our data show that thrust faulting with the same shortening direction initiated ~60 km farther north ca. 22 Ma in the Laji Shan (Fig. 3A). Third, and most notably, our data suggest that the primary direction of contraction in the composite Laji-Jishi Shan changed >45° ca. 13 Ma with the initiation of east-west shortening of the Jishi Shan (Fig. 3B). Furthermore, climate records from Neogene basin fills on either side of the Jishi Shan show development of a rain shadow due to surface uplift of the range by 11 Ma, but not before 16 Ma (Hough et al., 2011).

Temporal variations in the nature and orientation of range growth in northeastern Tibet provide a time series of how sustained, far-field India-Asia convergence was manifested near the margin of the plateau throughout the Cenozoic. Our study is unusual because it demonstrates that the currently conjoined Laji-Jishi Shan is in fact a composite structure that documents a change in the kinematic style of plateau deformation. NNE-SSW contraction since ca. 50 Ma in the West Qinling and since ca. 22 Ma in the Laji Shan occurred on a shortening trajectory that mimicked the larger India-Asia

convergence direction. By the Middle to Late Miocene, however, accelerated exhumation on north-south-trending structures in both the adjacent Jishi Shan (ca. 13 Ma) and nearby Liupan Shan (ca. 8 Ma) ~320 km to the east (Zheng et al., 2006) suggests the onset of east-west contraction inducing localized shortening and range growth. This new phase of east-west contraction occurred contemporaneously with continued NNE-SSW contraction (e.g., Zheng et al., 2010). The Middle Miocene onset of east-west contraction may signal the start of the modern deformation regime in northeastern Tibet, where shortening is coupled to strike-slip motion in a complex regional stepover between the Kunlun and Haiyuan left-lateral faults that includes diversely oriented subsidiary faults such as the Jishi Shan thrust fault (Duvall and Clark, 2010).

The development of new east-vergent thrust faults in northeastern Tibet that we document to have initiated by ca. 13 Ma coincides with the onset of a suite of significant phenomena in Tibet and its surroundings that collectively herald a transition to a new mode of plateau deformation. These phenomena include (1) the onset of east-west extension in the plateau interior at 14–8 Ma (e.g., Blisniuk et al., 2001); (2) expansion of the southeastern plateau margin after 13–11 Ma (e.g., Clark et al., 2005); (3) deceleration of strike-slip motion and acceleration of distributed shortening in northern Tibet since 18–15 Ma (e.g., Ritts et al., 2008); and (4) 40% slowing of India-Asia convergence rates between 20 and 11 Ma (Molnar and Stock, 2009). The relationship between these phenomena is debatable, but several potential geodynamic drivers for a Middle Miocene plateau-wide reorganization of deformation can be posited. Incipient lower crustal flow could link extension in the plateau interior with deformation on its margins (Royden et al., 2008). Alternatively, removal of mantle lithosphere beneath some portion of Tibet would incite initiation or change in the style of deformation on the plateau margins (e.g., England and Houseman, 1989). On the other hand, Tibetan deformation patterns since the Middle Miocene may be explained more simply by the progressive confinement of Tibetan crustal thickening against rigid crustal blocks to the north that cause deformation to be funneled toward the unconfined eastern margin. Minor eastward expansion of faulting, however, suggests that this is unlikely. The data in this paper argue that any viable model must honor a Middle Miocene reorganization of deformation in northeastern Tibet with the inception of east-west contraction.

ACKNOWLEDGMENTS

This work was supported by the U.S. National Science Foundation (NSF) Continental Dynamics program (grant EAR-0507431), a NSF graduate research fellowship to Lease, and the Chinese National Science Foundation (40234040, 40702028). We thank L. Hedges, P. O'Sullivan, and P. Zhang for assistance, plus E. Cowgill and an anonymous reviewer.

REFERENCES CITED

- Blisniuk, P.M., Hacker, B.R., Glodny, J., Ratschbacher, L., Bi, S.W., Wu, Z.H., McWilliams, M.O., and Calvert, A., 2001, Normal faulting in central Tibet since at least 13.5 Myr ago: *Nature*, v. 412, no. 6847, p. 628–632, doi: 10.1038/35088045.
- Clark, M.K., House, M.A., Royden, L.H., Whipple, K.X., Burchfiel, B.C., Zhang, X., and Tang, W., 2005, Late Cenozoic uplift of southeastern Tibet: *Geology*, v. 33, p. 525–528, doi: 10.1130/G21265.1.
- Clark, M.K., Farley, K.A., Zheng, D., Wang, Z.C., and Duvall, A., 2010, Early Cenozoic faulting on the northern Tibetan Plateau margin from apatite (U-Th)/He ages: *Earth and Planetary Science Letters*, v. 296, p. 78–88, doi: 10.1016/j.epsl.2010.04.051.
- Dewey, J.F., 1988, Extensional collapse of orogens: *Tectonics*, v. 7, p. 1123–1139, doi: 10.1029/TC007i006p01123.
- Duvall, A.R., and Clark, M.K., 2010, Dissipation of fast strike-slip faulting within and beyond northeastern Tibet: *Geology*, v. 38, p. 223–226, doi: 10.1130/G30711.1.
- England, P., and Houseman, G., 1989, Extension during continental convergence, with application to the Tibetan Plateau: *Journal of Geophysical Research*, v. 94, p. 17,561–17,579, doi: 10.1029/JB094iB12p17561.
- Flowers, R.M., Ketcham, R.A., Shuster, D.L., and Farley, K.A., 2009, Apatite (U-Th)/He thermochronometry using a radiation damage accumulation and annealing model: *Geochimica et Cosmochimica Acta*, v. 73, p. 2347–2365, doi: 10.1016/j.gca.2009.01.015.
- Hough, B.G., Garzzone, C.N., Wang, Z.C., Lease, R.O., Burbank, D.W., and Yuan, D.Y., 2011, Stable isotope evidence for topographic growth and basin segmentation: Implications for the evolution of the NE Tibetan plateau: *Geological Society of America Bulletin*, v. 123, p. 168–185, doi: 10.1130/B30090.1.
- Hu, S.B., He, L.J., and Wang, J.Y., 2000, Heat flow in the continental area of China: A new data set: *Earth and Planetary Science Letters*, v. 179, p. 407–419, doi: 10.1016/S0012-821X(00)00126-6.
- Ketcham, R.A., 2005, Forward and inverse modeling of low-temperature thermochronometry data: *Reviews in Mineralogy and Geochemistry*, v. 58, no. 1, p. 275–314, doi: 10.2138/rmg.2005.58.11.
- Ketcham, R.A., Carter, A., Donelick, R.A., Barbarand, J., and Hurford, A.J., 2007, Improved modeling of fission-track annealing in apatite: *American Mineralogist*, v. 92, p. 799–810, doi: 10.2138/am.2007.2281.
- Molnar, P., and Lyon-Caen, H., 1989, Fault plane solutions of earthquakes and active tectonics of

- the Tibetan Plateau and its margins: *Geophysical Journal International*, v. 99, p. 123–154, doi: 10.1111/j.1365-246X.1989.tb02020.x.
- Molnar, P., and Stock, J.M., 2009, Slowing of India's convergence with Eurasia since 20 Ma and its implications for Tibetan mantle dynamics: *Tectonics*, v. 28, TC3001, doi: 10.1029/2008TC002271.
- Qinghai Bureau of Geology and Mineral Resources, 1991, Regional geology of the Qinghai Province: Beijing, Geological Publishing House, 662 p.
- Ritts, B.D., Yue, Y.J., Graham, S.A., Sobel, E.R., Abbink, O.A., and Stockli, D., 2008, From sea level to high elevation in 15 million years: Uplift history of the northern Tibetan Plateau margin in the Altun Shan: *American Journal of Science*, v. 308, p. 657–678, doi: 10.2475/05.2008.01.
- Rowley, D.B., 1996, Age of initiation of collision between India and Asia: A review of stratigraphic data: *Earth and Planetary Science Letters*, v. 145, p. 1–13, doi: 10.1016/S0012-821X(96)00201-4.
- Royden, L.H., Burchfiel, B.C., and van der Hilst, R.D., 2008, The geological evolution of the Tibetan plateau: *Science*, v. 321, no. 5892, p. 1054–1058, doi: 10.1126/science.1155371.
- Tapponnier, P., Peltzer, G., Ledain, A.Y., Armijo, R., and Cobbold, P., 1982, Propagating extrusion tectonics in Asia—New insights from simple experiments with plasticine: *Geology*, v. 10, p. 611–616, doi: 10.1130/0091-7613(1982)10<611:PETIAN>2.0.CO;2.
- Yin, A., and Harrison, T.M., 2000, Geologic evolution of the Himalayan-Tibetan orogen: *Annual Review of Earth and Planetary Sciences*, v. 28, p. 211–280, doi: 10.1146/annurev.earth.28.1.211.
- Yin, A., Rumelhart, P.E., Butler, R., Cowgill, E., Harrison, T.M., Foster, D.A., Ingersoll, R.V., Qing, Z., Wian-Qiang, Z., Xiao-Feng, W., Hanson, A., and Raza, A., 2002, Tectonic history of the Altyn Tagh fault system in northern Tibet inferred from Cenozoic sedimentation: *Geological Society of America Bulletin*, v. 114, p. 1257–1295, doi: 10.1130/0016-7606(2002)114<1257:THOTAT>2.0.CO;2.
- Zheng, D., Zhang, P.Z., Wan, J.L., Yuan, D.Y., Li, C.Y., Yin, G.M., Zhang, G.L., Wang, Z.C., Min, W., and Chen, J., 2006, Rapid exhumation at ~8 Ma on the Liupan Shan thrust fault from apatite fission-track thermochronology: Implications for growth of the northeastern Tibetan Plateau margin: *Earth and Planetary Science Letters*, v. 248, p. 198–208, doi: 10.1016/j.epsl.2006.05.023.
- Zheng, D., Clark, M.K., Zhang, P., Zheng, W., and Farley, K.A., 2010, Erosion, fault initiation and topographic growth of the North Qilian Shan (northern Tibetan Plateau): *Geosphere*, v. 6, p. 1–5, doi: 10.1130/GES00523.1.

Manuscript received 2 May 2010

Revised manuscript received 28 October 2010

Manuscript accepted 12 November 2010

Printed in USA